Change in Femur Shape during Postnatal Development and Growth of C57BL/6 Mice

Introduction: Disorders of skeletal development, including hip dysplasia, slipped capital femoral epiphysis, and Legg-Calve-Perthes disease, often involve deviations from a healthy femur shape. However, to date, the changes in femur shape during postnatal development have only been quantified in terms of 2-D radiological parameters and other metrics that are neither independent nor sufficient to characterize the entire 3-D surface[1]. The study of a variety of disorders and therapies of skeletal development may benefit from metrics to quantify the changes in bone shape that may affect or reflect growth or disease. Statistical shape modeling is a technique that has been used to compare different populations by describing the variation among landmarks; the shape of an object is described in terms of parameters (modes) defined for a set of training specimens[2,3,4]. The objectives of this study were to quantify and map changes in mouse femur shape during normal postnatal development and growth up to maturation (day 30) using statistical shape modeling techniques.

Methods: ***Samples & Imaging*** With IACUC approval, the left and right hindlimbs of thirteen C57BL/6 mice at 2 days (n=4), and 12, 24, and 30 days (n=3, each) of age were harvested and scanned using uCT (SkyScan 1076) at (9μm)[3]. ***Segmentation.*** Bone threshold values were determined by intensity histogram analysis of CT scans, and the cortical bone surface of the femur was segmented using Mimics (Materialise) with region growing and morphological and Boolean operations to yield two surfaces of interest, the femur between the epiphyseal plates (diaphysis) and the whole femur (**Fig.1**). Results were validated visually based on *a priori* knowledge of general hip morphology. 3-D surfaces of the femur were reconstructed and exported as point clouds. ***Registration.*** Using MATLAB (Mathworks), right femurs were flipped in orientation to match their corresponding left femurs, and all samples were rigidly registered and isotropically scaled to a reference shape defined as the largest-volume sample. ***Active Shape Modeling.*** Using custom MATAB code, an atlas shape was constructed for both surfaces of interest by iterative distance-transform blending of rigidly registered training shapes and applying the mean non-rigid transformation to the training set. Three different scenarios were modeled: 500 landmark coordinates were defined on the atlas shape and automatically extrapolated to the atlas-aligned training shapes by non-rigid transformation to model the diaphysis and whole femur, and the whole femur landmark set was constrained to 381 landmark points proximal to a plane perpendicular to the shaft axis at the crest of the third trochanter to model the proximal femur. Landmark points were Procrustes aligned to remove global shape variance, and principal component analysis[5] was performed to find modes of variation that could cumulatively explain >90% of the variance in local femur shape. Specimens at two days did not have a distinguishable proximal femur shape and thus were omitted from the final whole and proximal femur models. ***Statistics.*** Agreement between consecutive atlas iterations from blended training shapes was determined using Cohen's kappa, which measures the overlap in voxels after accounting for chance. Correlation between mode parameters and age of the specimen was measured using linear regression, and differences in mode parameters between age points were assessed by a one-way ANOVA with post-hoc Tukey.

Results: The overall size and shape of the mouse femur changed significantly over the evaluated growth period. Average lengthening rate for femur from the proximal end to the distal epiphyseal plate was 0.27 mm per day (**Fig.2**).

Over two iterations of blending registered training shapes, kappa agreement between consecutive atlas iterations for the diaphysis model increased from 68.2% to 94.8% while over four iterations kappa increased from 72.6%, 97.1%, 97.4% to 98.1% for the atlas used to model the whole and proximal

femur.

Two modes of variation described 90% of the shape variability in the diaphysis of the femur. Characteristics of the modes are shown in **Table 1**. Mode 1 mainly described changes in the length:width ratio of the femur (**Fig.3A**). Mode 2 involved fine-tuning of the femoral neck and head shape (**Fig.3B**).

In the whole femur shape, two modes of variation also described 90% of the shape variability within the training set. Characteristics of the modes are shown in **Table 2**. Mode 1 mainly described changes in the femoral head size and length:width ratio of the femur (**Fig.4A**). Mode 2 involved fine-tuning of the femoral head shape (**Fig.4B**).

Specific variations in proximal femur shape, especially around the femoral head, emerged from eleven modes of variation that described 90% of the shape variability within the samples. Characteristics of the modes are shown in **Table 3**. Mode 1 mainly described the increasing sphericity of the femoral head and protrusion of the greater trochanter relative to the trochanteric fossa (**Fig.5A**). Mode 2 involved fine-tuning of the femoral neck and head shape (**Fig.5B**).

For all three model scenarios, mode 1 was highly correlated with age, and mode 1 parameters were significantly different at all age points ($p<0.001$).

Discussion: The modes calculated from this image data set capture a number of key changes in 3-D femur shape that occur in the mouse within the first 30 days after birth. For both the diaphysis and whole femur models, it appeared that the increase in the length-to-width ratio (elongation) of the shaft over the postnatal age span dominated the overall shape variance, obscuring more subtle shape changes in the proximal femur. Selecting for proximal femur landmarks resulted in a model which required many more modes of variation to explain >90% variance. The regions of shape variation in the proximal femur model along the different modes were consistent with regional growth zones at the longitudinal growth plate, femoral neck isthmus, and trochanteric growth plate[6]. Overall, the femur grew proportionally in length, implying that growth plates of the proximal femur were active in a coordinated manner. Future expansion and application of this approach, for example examining the mutual shape changes of the acetabulum and femoral head, could reveal insights about variations in growth plate activity that occurs during normal and abnormal development.

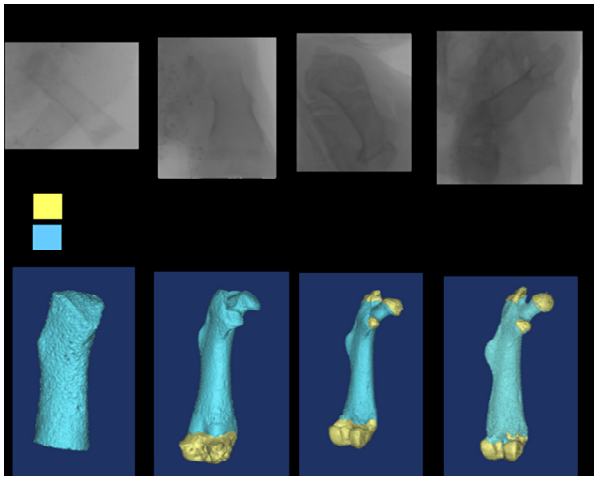

Figure 1: Segmentation of micro-CT scans of C57BL/6 at four age points (2, 12, 24, and 30 days) using region growing and morphological operation in Mimics (Materialise) of the outer cortical bone surface yielded two regions of interest, the diaphysis with cancellous bone filled in (cyan) and the epiphysis and

metaphysis with the growth plate junction filled in (yellow).

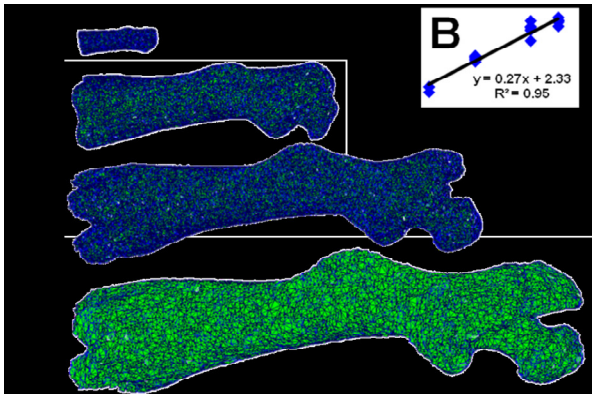

Figure 2: A) Representative mouse femora rigidly aligned in the same orientation at postnatal days 2, 12, 24, and 30, showing the development of trochanters and femoral head and B) lengthening rate of the femur.

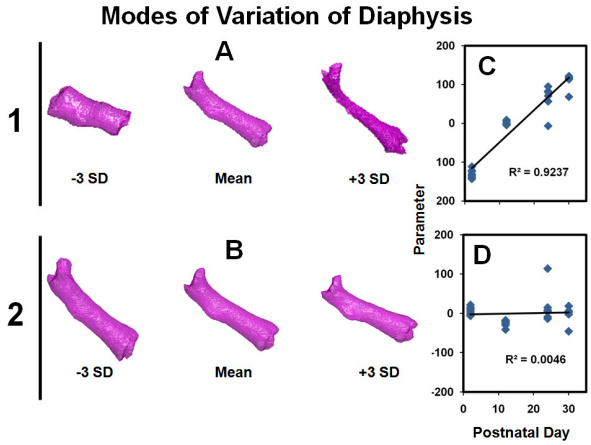

Figure 3: Contributions of shape change from the two principal modes of variation of the diaphysis. Mean shape ± 3 SD describe changes in A) femur length:width ratio, B) femoral head shape, and C-D) shows the distribution of parameters for each age group.

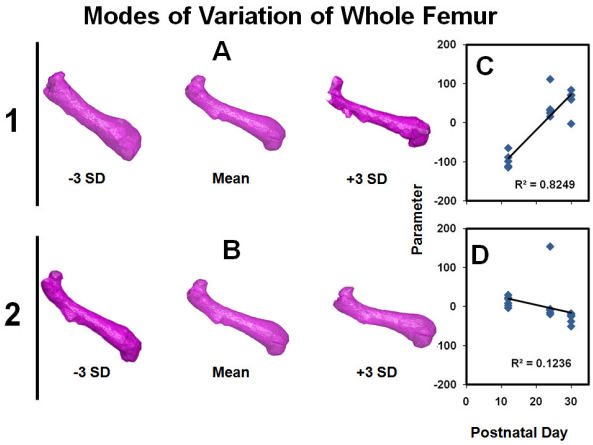

Figure 4: Contributions of shape change from the two principal modes of variation. Mean shape ± 3 SD describe changes in A) relative femoral head size and femur length:width ratio, B) femoral head shape, and C-D) shows the distribution of parameters for each age group.

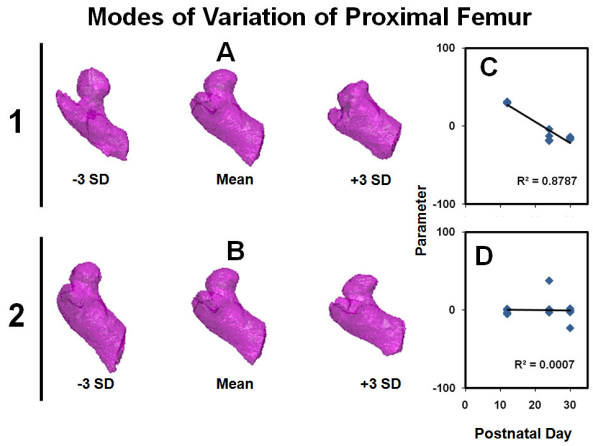

Figure 5: Contributions of shape change from the first three of eleven principal modes of variation of the proximal femur. Mean shape ± 3 SD describe changes in A) sphericity of femoral head and protrusion of greater trochanter, B) femoral head and neck shape. D-F) shows the distribution of parameters for each age group.

Mode	% Explained Variance	Postnatal					
		12	24	30			
1	69	-98.10	±19.1*	40.78	±35.3*	57.32	±30.6*
2	22	13.31	±12.8	15.85	±67.9	-29.15	±12.7

Table

Mode	% Explained Variance	Postnata					
		12	24	30			
1	53	30.53	±0.7*	-15.03	±6.0*	-15.49	±1.1*
2	13	-1.67	±2.8	6.05	±15.6	-4.38	±9.2
3	7	-0.45	±2.3	1.67	±6.7	-1.22	±12.8
4	4	0.58	±1.6	4.04	±6.2	-4.62	±6.0
5	3	0.05	±4.2	-2.55	±5.8	2.50	±5.0
6	3	0.20	±4.5	-1.25	±5.6	1.05	±5.2
7	2	-0.03	±5.9	-0.02	±3.8	0.05	±5.2
8	2	-0.14	±2.1	-0.25	±6.2	0.39	±5.1
9	2	-0.15	±3.7	-0.93	±4.5	1.08	±5.3
10	2	0.00	±3.0	0.51	±4.0	-0.50	±5.9
11	2	-0.03	±2.2	-0.95	±4.1	0.98	±5.9

ReferencesReferences

1. Than P, Sillinger T, Kranicz J, Bellyei A. Radiographic parameters of the hip joint from birth to adolescence. Pediatr Radiol. 2004;34(3):237-44.

2. Cootes TF, Taylor CJ, Cooper DH, Graham J. Active shape models - their training and application. Computer Vision and Image Understanding. 1995;61:38-59.

3. Gregory JS, Waarsing JH, Day J, Pols HA, Reijman M, Weinans H, et al. Early identification of radiographic osteoarthritis of the hip using an active shape model to quantify changes in bone morphometric features: can hip shape tell us anything about the progression of osteoarthritis? Arthritis Rheum. 2007;56(11):3634-43.

4. Frangi AF, Rueckert D, Schnabel JA, Niessen WJ. Automatic construction of multiple-object three-dimensional statistical shape models: application to cardiac modeling. IEEE Trans Med Imaging. 2002;21(9):1151-66.

5. Hamarneh G, Abu-Gharbieh R, Gustavsson T, editors. Review - Active Shape Models - Part I: Modeling Shape and Gray Level Variation. Swedish Symposium on Image Analysis; 1998.

6. Lee MC, Eberson CP. Growth and development of the child's hip. Orthop Clin North Am. 2006;37(2):119-32.

Acknowledgements: HHMI, NIH, NSF, UCSD-PRIME